

Betalain and anthocyanin dye-sensitized solar cells

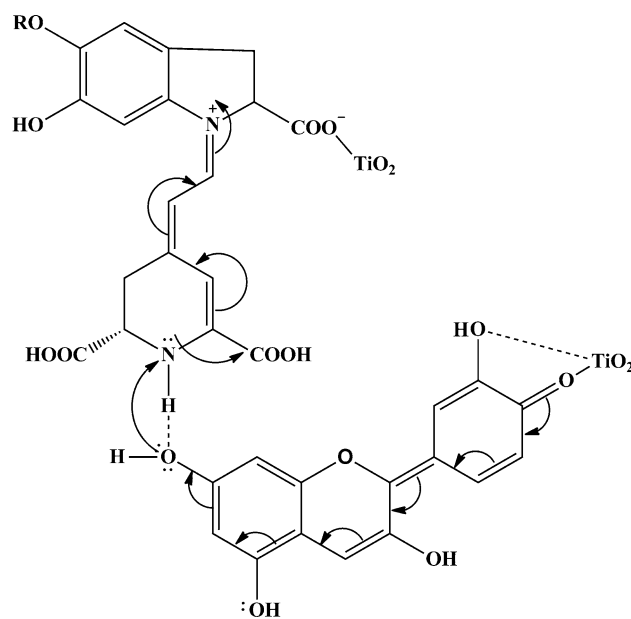
Raja Ramamoorthy¹ · Natarajan Radha² · Govindaraj Maheswari³ · Sambandam Anandan⁴ · Subbaiah Manoharan⁴ · Rayar Victor Williams¹

Received: 13 January 2016 / Accepted: 23 May 2016 / Published online: 4 June 2016
© Springer Science+Business Media Dordrecht 2016

Abstract In the present work, the mechanism behind the functioning of the eco-friendly dye-sensitized solar cell was explored. Dye-sensitized solar cells were fabricated using natural dyes extracted from common pear (*Opuntia dillenii*) and red tamarind (*Tamarindus indica*), and 1:1 mixture. Betalain and anthocyanin were identified as the main pigments that sensitize the semiconductor TiO₂ film. The best conversion efficiency of 0.47 % was achieved from betalain dyes and 0.14 % from anthocyanin dye-sensitized solar cell [under standard Air Mass 1.5 illumination (85 mW cm⁻²)]. The mixture of dye (1:1 mixture) adsorbed onto TiO₂ exhibited an efficiency of 0.20 %. The light absorption behavior of extracted dyes was studied using ultraviolet–visible analysis. The influence of the binding nature of the dyes with TiO₂ surface on the efficiency of the solar cells was analyzed through Fourier transform infra-red analysis. The electrochemical impedance spectroscopy was used to find out the internal charge transfer resistance of the cells. The device incident photon-to-current efficiency was obtained from 5 to 25 % for different natural dyes and found to coincide with the

photocurrent–voltage characteristics and electrochemical impedance spectroscopy analysis.

Graphical Abstract



✉ Rayar Victor Williams
rvwi@yahoo.com

- ¹ Department of Physics, St. Joseph's College, Tiruchirappalli 620 002, India
- ² Post Graduate and Research Department of Chemistry, Seethalakshmi Ramaswami College, Tiruchirappalli 620 002, India
- ³ Department of Physics, Cauvery College for Women, Tiruchirappalli 620 018, India
- ⁴ Nanomaterials and Solar Energy Conversion Lab, Department of Chemistry, National Institute of Technology, Tiruchirappalli 620 015, India

Keywords Dye-sensitized solar cell · Natural dyes · Betalain · Anthocyanin · TiO₂

1 Introduction

The conversion of solar energy to electricity appears as one of the technologies that can replace fossil fuels. Dye-sensitized solar cell (DSSC) is one of the serious competitors to solid state junction devices [1]. DSSC is composed of a

dye-sensitized nanocrystalline porous wide band gap semiconductor electrode, a counter electrode, and an electrolyte containing redox ions. The performance of DSSCs mainly depends on the dye used as the sensitizer [2]. Intense light absorption in the visible region and anchorage of the dye to the surface of a wide band gap semiconductor (titanium dioxide) are the important features that determine the efficiency of a cell [3]. The most efficient dye-sensitized solar cell is based on ruthenium metal complexes with a high solar harvesting efficiency of ~12 %. Intensive charge transfer in the whole visible region, long-excited life time of charge carriers, and highly efficient metal-to-ligand charge transfer kinetics have been identified as the causes of high efficiency [4]. Since ruthenium complexes are not eco-friendly, natural dyes that are cheap and abundant are preferred as sensitizers [5, 6]. Improvement in solar energy to electrical energy conversion efficiency using mixture of dye has been reported [7, 8]. Dyes having functional groups of –COOH or –OH that bind with TiO₂ nanoparticles via metal complexation provoke the electron transfer from the dye molecules to the conduction band of TiO₂ [9, 10].

Betalains are a class of red–violet (betacyanins) and yellow (betaxanthins) pigments that are present in plants of Caryophyllales [11]. The most promising sources of betalain are red beet root, amaranthus, and common pear—*Opuntia dillenii* (*O. dillenii*), a member of the family Cactacea [12, 13]. Anthocyanin pigments are responsible for the coloration of flowers, fruits, stems, leaves, and roots of plants that are present in blackberries, mango, and red tamarind—*Tamarindus indica* (*T. indica*) [14, 15]. Both betalain and anthocyanin dyes are known to absorb light in the visible region [16].

Recently many have investigated the dye-sensitized solar cells using betalain and anthocyanin dyes in different perspective. Gokilamani et al. [17] suggested that betalain dye extract from *Basella alba rubra* is an alternative source to construct natural dye-sensitized solar cells. They concluded that TiO₂ film annealed at 500 °C offered better conversion efficiency of 0.70 % due to better crystalline nature of the thin film. Reeza Hemmatzadeh and Ahmad Mohammadi used acidified ethanol and water mixture as a solvent to extract betalain dye from *Pastinaca Sativa* and *Beta vulgaris* and a fill factor of 0.95 was achieved. They reported that the acidity of the extracting solvent influences the extraction of various dyes which leads to better adsorption of dye molecules [18]. The betalain dye extract from *Bougainvillea glabra* by Kamin Uthman Isah showed a better conversion efficiency of 0.90 % using the dye at a pH of 3.0 which is due to recondensation of betalamic acid with amine groups that absorbs light in the visible region [19]. Sengupta et al. extracted betalain and chlorophyll dyes by ethanol from beet roots and spinach leaves

respectively. The mixture of these two dyes showed an efficiency of 0.29 %, whereas the individual dyes efficiency is of 0.19 % (betalain) and 0.14 % (chlorophyll dye). The better conversion was achieved due to the wider light absorption of mixture dye than the individual dyes [20]. Aparna et al. used betanin dye from beet roots to study the effect of Au doping on ZnO, thus improved the efficiency of the solar cell from 0.086 to 1.71 % [21].

Zularif Zolkepli et al. employed the ethanol extraction of anthocyanin dyes from *Tradescantia Spathacea* leaves and *Ixora Coccinea* petals to construct natural-based dye-sensitized solar cells. The mixture dye exhibited higher efficiency (0.80 %) than individual dyes (0.21 % for *T. Spathacea* and 0.56 % for *I. Coccinea*) due to better adsorption on TiO₂ [22]. Adel et al. extracted three anthocyanin dyes like cyaniding, aurantiidin, and rosidin from blackberry, *hibiscus*, and rose, respectively, using ethanol as a solvent. They employed plasticized polymer, regular iodine, and liquid polymer electrolyte to study its effect on conversion efficiency. Blackberry dye gave the highest conversion efficiency of 0.76 % compared to 0.058 % for *hibiscus* and 0.04 % for rose in iodine-based electrolyte. The same dye gave an efficiency of 0.24 and 0.14 % for liquid and thin film polymer electrolyte. The higher conversion efficiency of liquid polymer electrolyte-based DSSC is due to better ionic conductivity than thin film polymer electrolyte [23]. Chien and Hsu studied anthocyanin dye-sensitized solar cells based on solvent pH, dye concentration, purification, and immersion time. The anthocyanin dye from red cabbage achieved better conversion efficiency of 1.5 % at pH 8 and the concentration of 3 mM. The unpurified dye exhibited higher efficiency than the purified dye based on wider light absorption. When the immersion times were varied from 2 min to 2 days, the higher efficiency of 1.33 % was achieved for the photo anode with 15 min of immersion time [24]. Anthocyanin dye was extracted from *Ixora Coccinea* using 6 different solvents like absolute ethanol, 70 % ethanol, acetone, dimethylformamide, dimethyl sulfoxide, and water. The dye extracted using 70 % ethanol helps the device to achieve high electron density that leads to better efficiency of 0.50 % [25]. The effect of co-pigments like malic acid and ascorbic acid in anthocyanin dye from Mangosteen pericarp was studied by Munawaroh et al. The co-pigmentation helped to protect the color retention of anthocyanin from degradation improving the efficiency from 0.19 % for anthocyanin to 0.30 % for anthocyanin + malic acid mixture. The anthocyanin + ascorbic acid exhibited an efficiency of 0.29 % [26]. The purified and unpurified anthocyanin dye extracted from black rice was used by Prima et al. The unpurified dye contain chlorophyll b as a co-pigment, improved the efficiency of DSSC from 1.31 to 2.17 %. The better light absorption of

mixture dye and the intermediate energy level of chlorophyll b between anthocyanin and TiO_2 are the reasons for improved efficiency of the device. Moreover, the presence of Mg^{+} inside the chlorophyll b acted as metal center that provided the transition character of metal-to-ligand charge transfer [27]. The acidified ethanol extraction of anthocyanin dyes from *Morus alba Lam* and *Striga hermonthica* were used by Reda et al. The higher anthocyanin content from *M. alba* gave a reasonable higher efficiency of 0.43 % than 0.34 % from *S. hermonthica* [28].

The novelty of the present work is the construction of dye-sensitized solar cells from the naturally occurring dyes such as betalain and anthocyanin. The dyes are extracted from *O. dillenii* and *T. indica* fruits in solvent and used for the first time to fabricate the DSSCs at room temperature. The primary pigments betalain and anthocyanin are mixed together for the first time and studied the effect of co-sensitization on TiO_2 that influences on the conversion efficiency. The optical behaviors of the dyes are characterized by UV–visible and FT-IR spectral measurements. The electrical (I – V characteristics) measurement is done using solar simulator under standard Air Mass 1.5 illumination (85 mW cm^{-2}). The electrochemical impedance and incident photon current efficiency analysis are performed to study the charge transport property and quantum conversion efficiency of the solar cells.

2 Experimental section

2.1 Materials

Fluorine-doped tin oxide (FTO) conducting glass (resistivity $7 \Omega^2$, transmittance $>80 \%$), TiO_2 powder (anatase, particle size $\sim 25 \text{ nm}$), Triton X-100, methanol, polyethylene glycol (M.W 10,000), hydrochloric acid, nitric acid (Sigma Aldrich), synthetic dye N719 (Ruthenizer 535 bis TBA), liquid electrolyte (Iodolyte AN-50), and platinum catalyst paste (Platisol T/SP, Solaronix) were used in the present work.

2.2 Preparation of TiO_2 photo anode and platinum counter electrode

FTO conductive glass sheets were cleaned in a detergent solution using an ultrasonic bath for 15 min, further rinsed with ethanol, distilled water, and finally air dried. The TiO_2 photo anode was prepared by doctor blade method [29]. TiO_2 powder (0.2 g), 0.1 M nitric acid solution (0.4 ml), and polyethylene glycol (0.08 g) were ground until a homogenous paste was formed. Non-ionic surfactant Triton X-100 (0.05 ml) was added to the colloidal suspension, ground for 30 min, and placed in an ultrasonic bath for an

hour. Adhesive tape was pasted on the conductive side of FTO substrate to fix the active area as 16 mm^2 ($4 \text{ mm} \times 4 \text{ mm}$). A few drops of TiO_2 suspension were applied to one edge of the substrate and a glass rod was used to spread the paste uniformly on FTO. The coated plate was air dried and sintered at $450 \text{ }^\circ\text{C}$ in an open air furnace for 30 min. The thickness of the TiO_2 film was found to be $\sim 12 \mu\text{m}$ by stylus technique. The counter electrode was prepared by coating the conductive side of FTO glass with platinum precursor paste using doctor blade method and sintered at $450 \text{ }^\circ\text{C}$ for 30 min. The prepared electrodes were kept in a vacuum desiccator until further use.

2.3 Preparation of dye sensitizer extracts

Methanol and HCl were mixed in the ratio of 99:1 and was used as the extracting solvent. Betalain dyes were extracted from cactus fruits (*O. dillenii*). The fruits were cut into small pieces, crushed, and immersed in the solvent for a few hours. A clear dye solution obtained by filtration was stored in a dark place.

Anthocyanin dyes were isolated from red tamarind (*T. indica*). 25 g of red tamarind pulp was blended with 100 ml of extracting solvent for 12 h. The dark-colored extract was filtered and stored under darkness in a desiccator. *O. dillenii* and *T. indica* extracts were mixed to obtain 1:1 mixture.

The N719 standard dye ($(\text{Bu}_4\text{N})_2[\text{Ru}(4\text{-carboxy},4'\text{-carboxylato-2,2'-bipyridine})_2(\text{NCS})_2]$) solution was obtained by dissolving 10 mg of dye powder in 25 ml of anhydrous ethanol.

2.4 Fabrication of dye-sensitized solar cell

TiO_2 electrodes were preheated to $80 \text{ }^\circ\text{C}$ and immersed into the prepared dye solutions. The DSSCs were assembled by placing dye-stained TiO_2 photo anode on platinum counter electrode, facing each other, and clipped together using the binder clips. A few drops of electrolyte solution were placed on the edges of the plate and allowed to diffuse between the plates by capillary action.

2.5 Measurements

The UV–visible absorption spectrum of the dyes and the mixture were recorded using UV–visible spectrophotometer (Perkin Elmer Lambda 35). The chemical characterization was done by FT-IR spectroscopy (Perkin Elmer spectrum RX-1). The thickness of the TiO_2 film was determined using a stylus profilometer (Mitutoyo SurfTest SJ-401). The photovoltaic test measurement of DSSCs was performed under 85 mW cm^{-2} light illumination using an

Autolab PGSTAT potentiostat/galvanostat-84610. The electrochemical impedance spectra were recorded under the same illumination with a frequency range from 0.1 Hz to 100 kHz, and the potential modulation was 10 mV. The applied bias potential was set at open-circuit voltage of the cell. Incident photon-to-current efficiency (IPCE) of the cells was measured using Oriel instruments with a 300 Watt Xenon light source (Newport corporation) with varying light wavelength of 300–700 nm at 5 nm interval.

3 Results and discussion

3.1 UV–visible absorption spectra

3.1.1 Solution spectra

The UV–visible absorption spectra of *O. dilleni*, *T. indica* extract, and the mixture are as shown in Fig. 1. In the spectrum of *O. dilleni* extract, the absorption maximum observed at 517 nm indicates the presence of betalain dyes [30]. The light absorption spectrum ranges from 450 to 675 nm with a small hump at 650 nm. The absorption spectrum of *T. indica* extract shows a maximum at 525 nm and ranges from 450 to 600 nm. At pH 1.0, anthocyanins strongly absorb the visible light from 520 to 600 nm [31], and there is a change in the absorption peak of *T. indica* extract compared to black rice, blue pea flower, and Calafate extract due to the addition of HCl acid during the extraction process [32–34]. The light absorption intensity of *T. indica* extract is higher than that of *O. dilleni* extract. The UV–visible spectrum of the mixture exhibits a maximum absorption at 530 nm. It is observed that the light absorption behavior of the mixture is not a linear superposition of the individual dyes. The absorption spectrum of

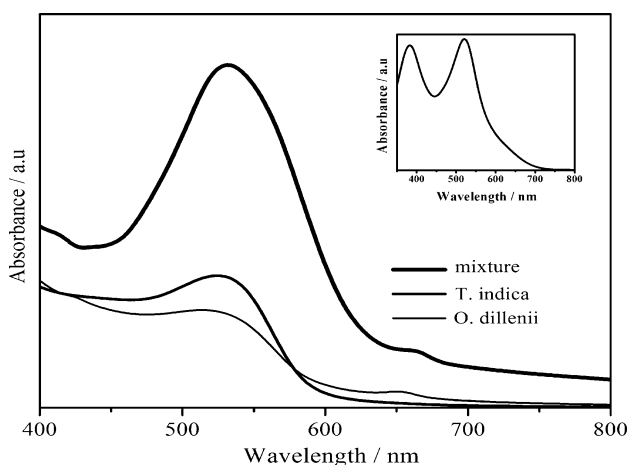


Fig. 1 UV–visible absorption spectra of *O. dilleni*, *T. indica* extract and the mixture. *Inset* standard N719 dye in ethanol

the mixture nearly matches with *T. indica* extract with a wider light absorption range and higher intensity and indicates the dominant behavior of anthocyanin dyes. A small hump at 675 nm indicates the presence of betalain dyes in the mixture. The absorption peak for betalain dyes may disappear due to low light absorption intensity than the anthocyanin dyes. The mixture covers light absorption from 425 to 700 nm. The wider and stronger light absorption behavior of mixture is expected to give the maximum photovoltaic conversion efficiency than the individual dyes. The standard N719 dye in ethanol is shown as an inset for comparison.

3.1.2 Film spectra

The UV–visible absorption spectra of all the dye-sensitized TiO₂ films are shown in Fig. 2. In the spectrum of *O. dilleni* extract-sensitized TiO₂ photo anode, the absorption maximum is red shifted to 525 nm indicating the interaction of betalain dye molecule with TiO₂, which is evident from the change in color from red to deep violet. The –COOH ligands on betalain dye molecule combine with hydroxyl group in TiO₂ to produce an ester-type linkage and boost electrons from the lowest unoccupied molecular orbital (LUMO) of the dye to the conduction band of TiO₂ to facilitate rapid electron transfer by coupling effect [35]. The possible binding between betalain dye molecule and TiO₂ is illustrated in Fig. 3. The absorption spectrum of *T. indica* dye-sensitized TiO₂ film exhibits a blue shift at 512 nm indicating the binding between anthocyanin dye molecules with TiO₂. The blue shift phenomenon is due to the dye aggregation in methanol the solvent used in dye extraction process [32]. Both the carbonyl and hydroxyl groups present in anthocyanin molecule bind to the surface

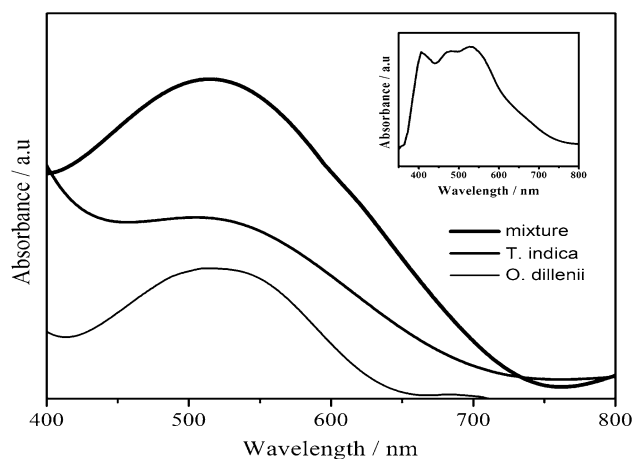


Fig. 2 UV–visible absorption spectra of *O. dilleni*, *T. indica* extract and the mixture-sensitized TiO₂ films. *Inset* standard N719 dye-sensitized TiO₂ film

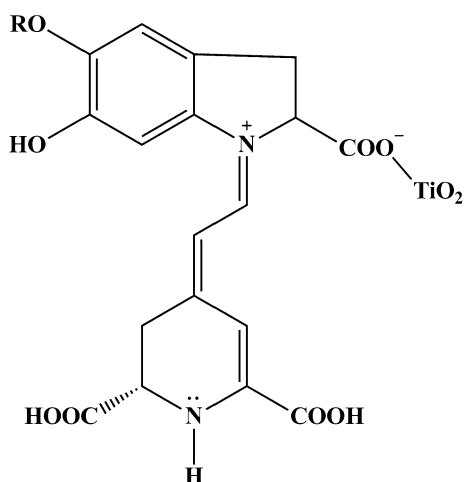


Fig. 3 Schematic representation of betalain dye molecule binding with TiO_2

of TiO_2 leading to photo conversion effect [36]. The possible binding of anthocyanin dye molecule with TiO_2 is illustrated in Fig. 4. In the UV–visible spectrum of the mixture-sensitized TiO_2 film, the blue shift at 517 nm indicates the binding between dyes and TiO_2 . Like anthocyanin dye-sensitized TiO_2 film, the mixture also exhibits a blue shift indicating the dominant behavior of anthocyanin dye molecule in the mixture. The absorption curves are smoother in the film spectra than the solution spectra, indicating that the dyes play a major role in the expansion of the light absorption behavior of TiO_2 in the visible region. It is expected from the expanded spectral region and intense absorption of visible light, the mixture may result in higher photo electric conversion efficiency compared to individual dyes. The standard N719-sensitized TiO_2 film is shown as an inset for comparison.

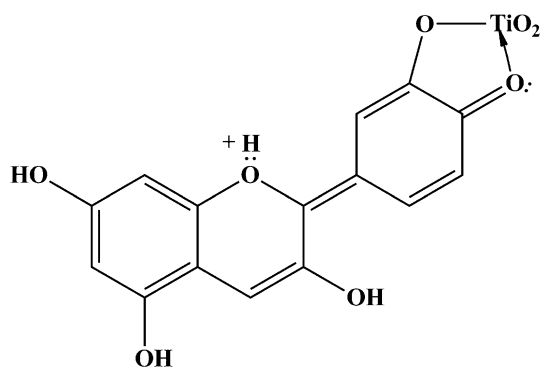


Fig. 4 Schematic representation of anthocyanin dye molecule binding with TiO_2

3.2 Fourier transform infra-red analysis

3.2.1 Solution spectra

The FT-IR spectra of *O. dillenii*, *T. indica* extract, and the mixture are shown in Fig. 5. From the spectrum of *O. dillenii* extract, the functional groups such as OH, NH, COOH, C=C, and phenyl ring vibrational modes are found. The OH and secondary NH stretching vibrations appear as sharp band at 3408 cm^{-1} indicating H bonding. The CH stretching vibrations at 2922 and 2860 cm^{-1} are due to aromatic and aliphatic CH groups, respectively. The $\text{C}=\text{N}^+$ stretching vibrations occur at 2360 cm^{-1} as a very sharp band. The CO group stretching vibrations occur at 1717 cm^{-1} while at 1616 cm^{-1} , CO in COO^- is found to be merged along with $\text{C}=\text{N}$ vibrations. At 1457 cm^{-1} , benzenoid ring stretching vibrations are seen. The sharp peak at 1373 cm^{-1} is due to C–N–C bending and C=N symmetric stretching vibrations. At 1219 cm^{-1} , C=N asymmetric stretching vibration occurs. The broad band at 1093 cm^{-1} arises due to C–O stretching vibration. The 1,2-disubstituted benzenoid ring bending is deciphered by the sharp peak at 771 cm^{-1} . The C–H and C–C bending vibrations occur as three sets at 666 , 595 , and 457 cm^{-1} .

In the FT-IR spectrum of *T. indica* extract, a broad band at 3410 cm^{-1} is due to the bonded OH groups. At 2956 cm^{-1} , CH stretching mode occurs as merged peak on the broad absorption spectrum and thus proves the presence of only aromatic CH group. The presence of $-\text{C}=\text{O}^+$ group is deciphered from the stretching vibrations at 2363 cm^{-1} . The broad absorption at 2078 cm^{-1} indicates further electron delocalization into adjacent rings. The broadening of bands at 1448 and 1283 cm^{-1} also represent several delocalized C=C bonds. The $\nu_{\text{C-O}}$ vibration at 1023 cm^{-1} is found as a combination band. The 1,4-disubstituted

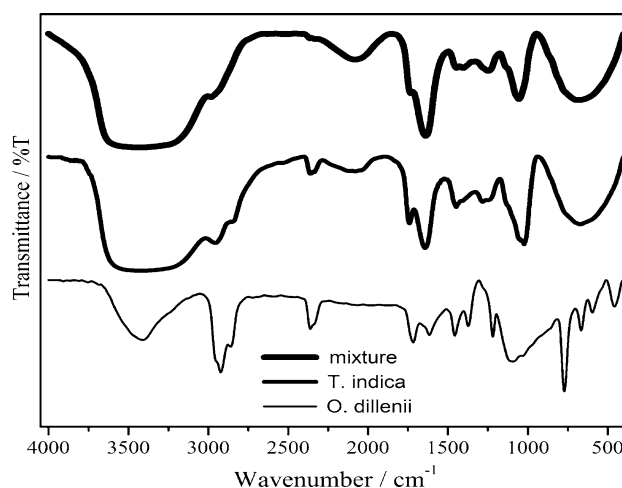


Fig. 5 FT-IR spectra of *O. dillenii*, *T. indica* extract and the mixture

benzene ring bending vibration at 676 cm^{-1} has also been broadened. The C=O group stretching vibrations occur at 1741 cm^{-1} . Since this group can also conjugate with ring double bonds, there is a strong stretching vibration at 1643 cm^{-1} due to C=C aromatic ring stretching vibrations.

In the FT-IR spectrum of the mixture of *O. dillenii* and *T. indica* extract, broad bands at 3432, 2080, 1249, 1055, and 678 cm^{-1} imply overlapping of stretching modes of several functional groups. The 3432 cm^{-1} band comprises NH and OH stretching vibration frequencies. The red shift (24 cm^{-1}) of NH bond indicates further H-bonding and electron shift from NH group to produce $\text{C}=\text{N}^+\text{H}$ structure in betalain. The OH group in anthocyanin at 3410 cm^{-1} has also red shifted to 3432 cm^{-1} , confirming H bonding at the site. There are almost similar shifts (22 cm^{-1}) for both NH of betalain and OH of anthocyanin moiety indicating strong binding. The disappearance of peak at 2360 cm^{-1} is due to the conjugation and resonance of mixture after the interaction between betalain and anthocyanin dye molecules. The band at 2080 cm^{-1} may arise from $\text{C}=\text{O}^+$ of anthocyanin and $\text{C}=\text{N}^+$ of betalain dye molecules. The 1249 cm^{-1} visible band is broadened by C=C stretching vibration of anthocyanin and C=N symmetric stretching of betalain. At 1055 cm^{-1} , all the C–O stretching vibrations are merged. Similarly all bending vibrations coalesce together at 678 cm^{-1} . The band at 1732 cm^{-1} due to C=O group of anthocyanin and COOH group of betalain occurs as shoulder on the 1639 cm^{-1} band (C=N) indicating the binding between these groups. Twin bands appear at 1446 and 1406 cm^{-1} . The 1446 cm^{-1} band is due to C=C of aromatic rings in both anthocyanin (1447 cm^{-1}) and betalain (1457 cm^{-1}). The band at 1457 cm^{-1} of betalain has disappeared in the mixture and is replaced by a new band at 1406 cm^{-1} . In this region, electron delocalization in C=C groups can be deciphered. Since there is a new peak at 1406 cm^{-1} , equal in intensity to the 1446 cm^{-1} band, strong electron displacement between betalain and anthocyanin can be inferred.

3.2.2 Sensitized TiO_2 film spectra

In the FT-IR spectrum of the film sensitized with betalain dyes, the presence of free OH groups is evident from the broad band at $3600\text{--}3766\text{ cm}^{-1}$ (Fig. 6). The secondary NH vibration at 3310 cm^{-1} has blue shifted by 98 cm^{-1} compared to the solution spectrum. The CH stretching vibrations are found at $3100\text{--}3018$ and 2865 cm^{-1} . Various $\text{C}=\text{N}^+$ stretching vibrations in the film appear as multiple bands compared to the solution spectrum in the region 2606, 2471, 2295, 2195 cm^{-1} , and a sharp band at 2022 cm^{-1} implies the electron shifts from secondary NH to the $\text{C}=\text{N}^+$. In the C=O vibrational stretching region,

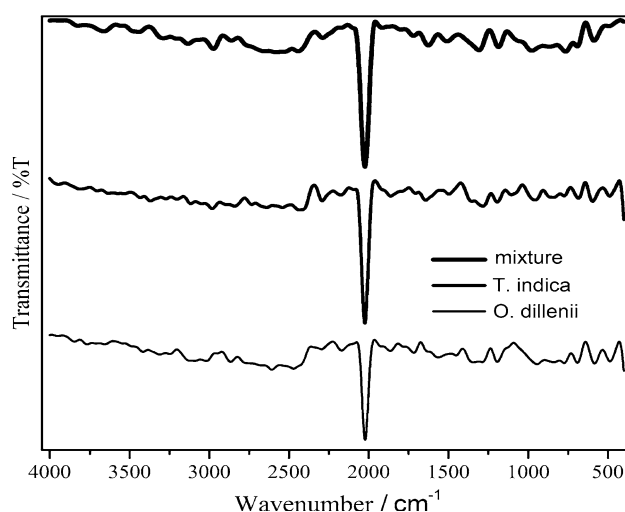


Fig. 6 FT-IR spectra of *O. dillenii*, *T. indica* extract and the mixture-sensitized TiO_2 films

besides the 1716 cm^{-1} band, a new band appears at 1864 cm^{-1} which may be due to bonding of COOH to TiO_2 surface. The C=C stretching of aromatic ring has blue shifted from 1616 to 1564 cm^{-1} . The peak at 1457 cm^{-1} found in solution has disappeared in the film spectrum. There is a blue shift of 1373 cm^{-1} vibration to 1343 cm^{-1} in the film which is the band for C–N–C bending vibration. The C–O vibration at 1219 and 1092 cm^{-1} has shifted to 1193 and 944 cm^{-1} , respectively, in the film. Several bending vibrations are found in the region of $773\text{--}486\text{ cm}^{-1}$.

The adsorption of anthocyanin onto TiO_2 film in the quinoid form depends on the existence of two –OH groups ortho to one another on the aromatic ring, a motif that in general leads to strong electronic coupling and rapid forward and reverse electron transfer due to the conjugated structure. These characteristics are observed in the FT-IR spectrum of anthocyanin-adsorbed TiO_2 film as shown in Fig. 6. OH groups in anthocyanin-adsorbed TiO_2 film are distinct at 3369, 3203, and 3116 cm^{-1} . All these are blue shifted compared to solution indicating electron delocalization in the free OH groups in the film. C–H stretching vibrations are red shifted by 25 cm^{-1} and found to be at 2981 and 2841 cm^{-1} . $\text{C}=\text{O}^+$ stretching modes are distinct and several bands are observed at 2640, 2541, 2435, 2292, and 2175 cm^{-1} , all these are coalesced in liquid sample as a broad band at 2363 and 2078 cm^{-1} . C=O stretching vibration observed at 1741 cm^{-1} in the liquid sample is red shifted to 1862 cm^{-1} while no shift is found for 1643 cm^{-1} band. C=C stretching is red shifted in film from 1447 to 1497 cm^{-1} . C–O vibration at 1023 cm^{-1} in solution is also red shifted to 1105 and 1194 cm^{-1} . Bending vibrations occur distinctly at 956, 841, 774, 684, 595, and 489 cm^{-1} in the film. Binding of C=O and OH groups to TiO_2 is

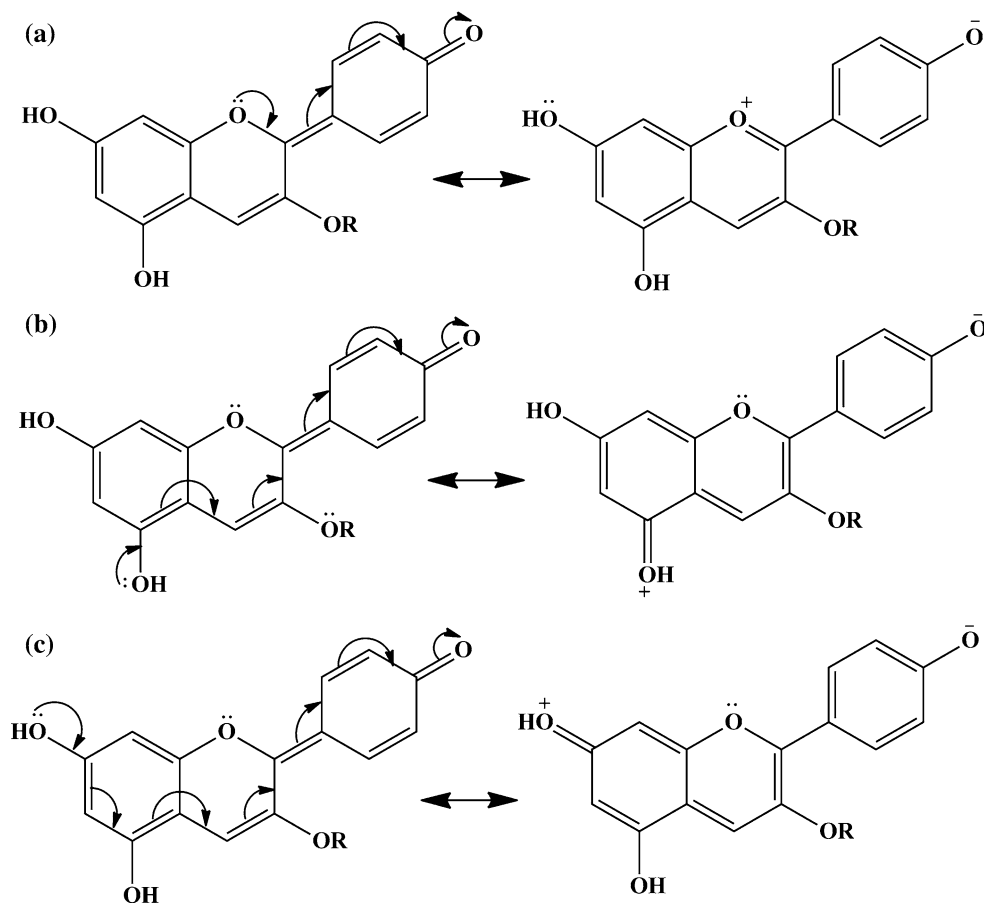
indicated by red shifts of C=O stretching vibration and blue shift of OH stretching mode. The schematic representation of electron delocalization in anthocyanin dye molecule is shown in Fig. 7a–c.

In the FT-IR spectrum of the film prepared from the mixture, O–H and NH bands of the mixture, several stretching vibrational bands are observed at 3662, 3442, and 3133 cm^{-1} . The NH band at 3432 cm^{-1} has red shifted to 3442 cm^{-1} ($\Delta\nu = 10 \text{ cm}^{-1}$). The C–H vibrations are distinct at 2973 and 2860 cm^{-1} . In the C=N⁺ region, several separate bands are found at 2580, 2443, 2289, and 2023 cm^{-1} . The broad band at 2080 cm^{-1} has red shifted at 2289 and blue shifted at 2023 cm^{-1} ($\Delta\nu = 109$ and 57 cm^{-1}). The C=O group appears at 1718 cm^{-1} which is blue shifted by $\Delta\nu$ of 15 cm^{-1} . The CO of COO⁻ group has blue shifted from 1639 to 1625 cm^{-1} ($\Delta\nu = 14 \text{ cm}^{-1}$). The C=C vibrations are found at 1508 cm^{-1} . The bands observed at 1449 and 1406 cm^{-1} in the solution spectra are absent. The C–N–C bending vibration is found in the film at 1308 cm^{-1} . The C–O stretching vibration at 1055 cm^{-1} has blue shifted to 977 cm^{-1} . The broad band at 678 cm^{-1}

due to bending vibrations appears separately in the film at 765, 691 and 586 cm^{-1} .

In the FT-IR spectra of all films, a sharp stretching absorption is found at 2020 cm^{-1} . When betalain dye molecules are bound to TiO₂ surface, a sharp vibration occurs at 2022 cm^{-1} . When anthocyanin dye molecules are bound to TiO₂, the vibration of TiO₂ occurs at 2024 cm^{-1} and for the mixture, TiO₂ stretch occurs at 2023 cm^{-1} . The intensity of the peak in *T. indica* extract is 0.6051 (%T = 24.82), for *O. dillenii* extract is 0.3459 (%T = 45.09) and for the mixture it is found to be 0.6206 (%T = 23.95). The increased intensity of the mixture in the film implies efficient interaction with TiO₂ surface. The strong interaction of the mixture to TiO₂ surface may be the cause of high solar power conversion efficiency expected in DSSCs. The purpose of investigating the FT-IR spectrum of the mixture is to ascertain the structure of the mixture solution responsible for harvesting the solar energy on the site of TiO₂. The various FT-IR spectral features are expressed in Fig. 6, and the electron shift in the mixture is shown in Fig. 8.

Fig. 7 Structure of the key component in *T. indica* extract (anthocyanin) in different resonating form



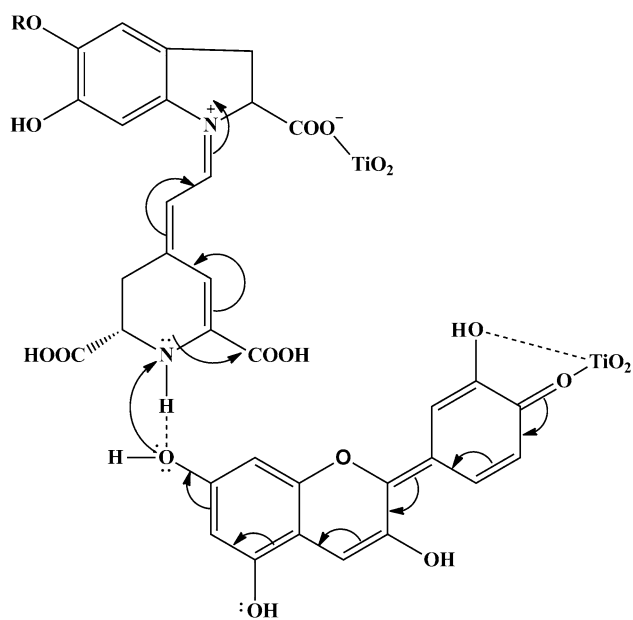


Fig. 8 Schematic representation of the mixture binding to TiO_2 surface

3.3 Photoelectrochemical behavior of DSSCs

3.3.1 Current–voltage characteristics

The photoelectrochemical behavior of the DSSCs using betalain, anthocyanin, and the mixture as a sensitizer is expressed in terms of open-circuit voltage (V_{oc}), short-circuit current (I_{sc}), maximum voltage (V_{max}), maximum current (I_{max}), fill factor (FF), and efficiency (η) is presented in Table 1. DSSC prepared using betalain dyes is found to exhibit a maximum efficiency followed by the mixture and anthocyanin dye-sensitized solar cells. Betalain dye-sensitized solar cells have shown an efficiency of 0.47 %. Oprea et al. [37] have shown that the acidified methanol extraction of betalain dyes from beet root extract shows an efficiency of 0.04 %, after the removal of betaxanthin and other impurities. The extract of betalain dyes from bougainvillea and beet root has been used by Narayan and Sandquist to construct DSSCs. The device exhibited an efficiency of 0.38 and 2.7 % for bougainvillea and beet root extract, respectively [38, 39].

In the present work, the DSSC fabricated using anthocyanin dyes from *T. indica* as sensitizer shows an efficiency of 0.14 %. DSSC efficiency of 0.56 and 0.17 % from black berry and red cabbage, respectively, is shown by Hao et al. [32] and Cherephy et al. [40]. Hemalatha et al. [41] has shown an efficiency of 0.29 % on DSSCs using raw ethanol extraction of anthocyanin dyes from *Rosa chinensis*. Calogero et al. using concentrated red Sicilian orange juice have observed an improved efficiency of 1.01 % than the acidified extracts (pH < 2.0) which may be due to high the quantity of anthocyanin. Generally anthocyanin-based DSSCs show the efficiency ranging from 0.1 to 1.0 % [42].

The fabrication of DSSC from the mixture shows a moderate efficiency (0.20 %) between the pure components and has no synergetic effect on it. The extraction of anthocyanin dyes from rosella and blue pea flower by Wongcharee et al. [33] gives a higher efficiency of 0.37 % from rosella extract than the mixture dye solution ($\eta = 0.15$ %). A mixture dye of chlorophyll and anthocyanin from pomegranate leaf and mulberry extract shows a higher efficiency of about 0.72 % than the individual dye [43]. Chang et al. have used chlorophyll extracts from ipomoea leaves and spinach and the mixture to study the sensitizing efficiency in DSSCs. The dye from ipomoea leaves shows an efficiency of 0.31 % under extraction temperature of 50 °C and pH value of 1.0 which is reported to be higher than spinach extract and the mixture [44]. Furukawa et al. have extracted dyes from red cabbage and curcumin and an efficiency of 0.61 % has been achieved for mixture dye [45]. Several reports on DSSCs show that the mixture performed well over the individual dyes, and vice versa for a few extracts. The efficiency of the DSSCs depends on the kind of dyes, difference in extraction temperature, pH, and the methods involved in anode preparation.

In the UV–visible spectra of betalain and anthocyanin dyes, it is observed that both the dyes have absorption peak at ~ 525 nm. The betalain dye-sensitized solar cell exhibits the maximum efficiency over anthocyanin dye-sensitized solar cells. It is due to the presence of carboxylic functional group ($-\text{COOH}$) in the betalain which is a good sensitizer than $-\text{OH}$ group in anthocyanin. Further the oxidation potential of betalain dyes has been found to be similar to

Table 1 Photocurrent–voltage parameters of DSSCs fabricated with *O. dillenii*, *T. indica* extract and the mixture

Extract sources	I_{sc} (mA cm^{-2})	V_{oc} (V)	FF	η (%)
<i>O. dillenii</i>	1.09	0.521	0.69	0.47
<i>T. indica</i>	0.35	0.532	0.67	0.14
Mixture dye	0.51	0.529	0.64	0.20
Layer by layer co-sensitization	0.24	0.507	0.71	0.09
N719	17.34	0.674	0.51	7.08

that of ruthenium polypyridyl complexes. The strong binding nature of betalain dyes with TiO_2 surface and an efficient dye regeneration by iodine/iodide redox couple have been reported by earlier works [37, 46]. Anthocyanin molecules containing glucose units may affect the effective bond formation on TiO_2 surface leading to slow electron transfer to the conduction band of TiO_2 .

When TiO_2 photo anode is sensitized with the mixture, both betalain and anthocyanin molecules are adsorbed onto TiO_2 surface. From the UV–visible spectrum, the major constituent of mixture dye is anthocyanin. When the mixture is used to sensitize TiO_2 , the blue shift phenomenon is observed similar to the anthocyanin dye-sensitized TiO_2 film indicating the dye aggregation. This is due to the attachment of OH functional group in anthocyanin with betalain dye molecule resulting in intermolecular interactions forming dye aggregation that is conformed through FT-IR analysis. The dye aggregation restricts the utilization of original properties of individual dye for efficient photo energy conversion. In aggregated or mixed state, a considerable amount of absorbed energy is utilized in thermal process than efficient charge separation [47]. This may lead to the lower efficiency of DSSC. At the same time, the addition of betalain dyes with anthocyanin dyes improves the efficiency of bare anthocyanin dye-based DSSC from 0.14 to 0.20 %. Thus in the present work, the attempt to use the mixture to fabricate DSSC shows I_{sc} of 0.51 mA cm^{-2} , V_{oc} of 0.529 V, and FF of 0.648. A slight increase in efficiency observed in the work may be due to the higher I_{sc} than anthocyanin-based DSSC.

Kumara et al. have shown that double layer co-sensitization of natural pigments can improve an overall efficiency of the DSSCs [41]. We have studied DSSCs using double layer co-sensitization of betalain and anthocyanin dyes. In this method, the TiO_2 photo anode is first sensitized with anthocyanin dyes followed by betalain for 7 h. The conversion efficiency η of 0.09 % with I_{sc} of 0.24 mA cm^{-2} , V_{oc} of 0.507 V, FF of 0.717, is, however, lower than all the other devices. This may be due to the fact that the initial adsorption of anthocyanin molecules on TiO_2 surface during the sensitizing process restricts the further adsorption of the betalain dyes. Hence optimizing the sensitizing time is necessary to improve the efficiency of DSSC based on layer by layer co-adsorption of two different dyes. The photovoltage–photocurrent density curves of the DSSCs are shown in Fig. 9. In order to compare the overall performance of natural DSSCs, N719 dye is used as reference dye and photovoltage–photocurrent density curve is shown as an inset. N719 dye shows an efficiency of 7.08 % with I_{sc} of 17.34 mA cm^{-2} , V_{oc} of 0.674 V, and FF of 0.51. The maximum overall performance of N719 dye may be due to the good electron

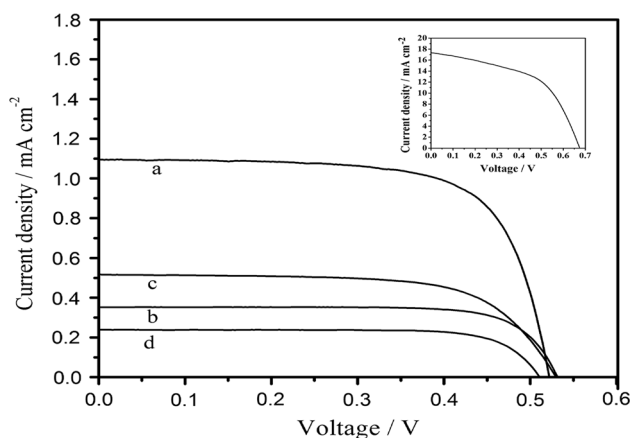


Fig. 9 Photocurrent–voltage curves for natural dye-sensitized solar cells fabricated using *a* *O. dillenii* extract, *b* *T. indica*, *c* the mixture, and *d* layer by layer co-sensitization. The I – V curve of standard N719 dye shown as an inset for comparison

injection property, longer electron life time, and wider light absorbing behavior [3].

3.3.2 Electrochemical impedance spectroscopy (EIS) analysis

The EIS is a powerful, informative, and nondestructive method to study the properties of interface and electron kinetics in DSSC. Generally EIS of a DSSC consists of three characteristic semicircles in the frequency range between 10^5 and 0.1 Hz. Three semicircles from Nyquist plot represents the impedance of the charge transfer resistance (R_{ct1}) on the Pt counter electrode at high-frequency region, the charge transport resistance (R_{ct2}) on the interface of the TiO_2 /dye/electrolyte at mid-frequency region, and diffusion in electrolyte (Z_N) at low-frequency region, respectively. The high-frequency interception on the real axis can be attributed to the sheet resistance (R_S) of TCO. So the total series resistance of a DSSC should be comprised four resistance values [48]. Since same Pt electrodes are used in all our experiments, the focus is on the resistance at the TiO_2 /dye/electrolyte interface. As shown in Fig. 10, the EIS spectra of all the devices exhibited only two semicircles and the semicircle of Z_N is not obvious and overlapped by R_{ct2} . The diameter of the semicircles in the plot is reduced which indicates a decrease in the interface layer resistance and an effective separation of photo generated electron hole pairs and fast interfacial charge transfer between TiO_2 matrix to TCO anode [49]. Among the four natural DSSCs the *O. dillenii* dye-sensitized solar cell exhibits lower R_{ct2} value followed by mixture dye and *T. indica* dye. The co-sensitization process affects the effective electron hole separation in the device and exhibits higher R_{ct2} value which is consistent with I – V characteristics. The difference

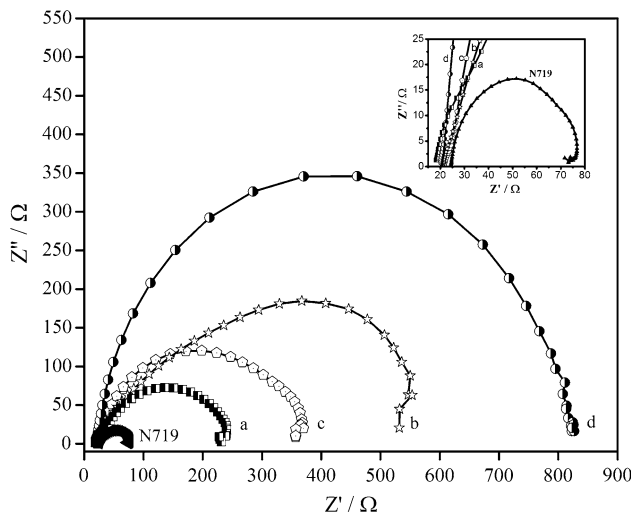


Fig. 10 Nyquist plots measured from EIS data for *a* *O. dillenii*, *b* *T. indica*, *c* the mixture-sensitized solar cells and *d* layer by layer co-sensitization process under irradiation of 85 mW cm^{-2} AM 1.5 at open-circuit voltage. *Inset* shows the Nyquist plot of N719 dye-sensitized solar cell under the same condition

in R_{ct2} can be associated with the binding between the dye molecules and TiO_2 . This may be due to the dye aggregation during the sensitizing process which leads to weaker binding and higher resistance which in turn gives lower I_{sc} to the device. This explains why the DSSC with co-sensitization leads to lower efficiency among all the devices. The inset shows the Nyquist plot of N719 dye-sensitized solar cell and the R_{ct2} value which is very much lower than the natural dye-based devices. The total internal resistance is inversely proportional to the photovoltaic performance of DSSCs, and this gives the reason for higher efficiency in commercial dyes. The R_s values of all the devices are alike and proved that all the devices were fabricated under similar conditions. The value of R_{ct2} depends on the dye used as the sensitizer and is summarized in Table 2.

Figure 11 illustrates the Bode plot of DSSCs sensitized with four natural dyes. It consists of two peaks: one peak at a mid-frequency and the other at high-frequency region which corresponds to the effective lifetime of electrons on

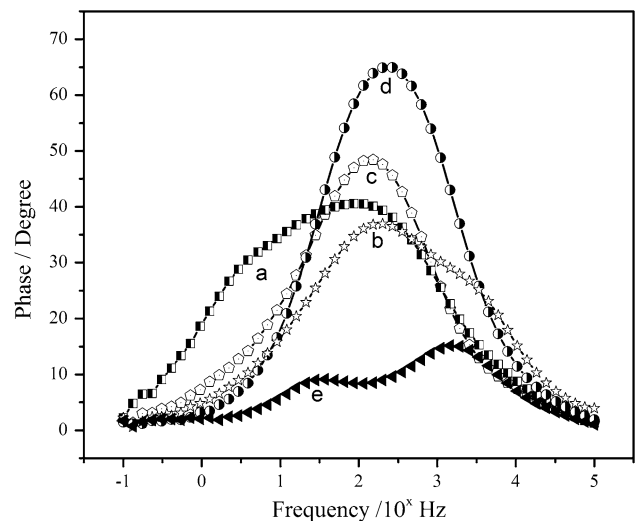


Fig. 11 Bode phase plots of DSSCs fabricated using *a* *O. dillenii*, *b* *T. indica*, *c* the mixture, *d* co-sensitization process, and *e* N719 dye

the $\text{TiO}_2/\text{dye}/\text{electrolyte}$ interface and the effective lifetime of electron on the Pt counter electrode, respectively. The peak frequencies are inversely proportional to electron life time [25]. Since the frequency at the high-frequency region is related to the charge transfer at the interface of electrolyte/Pt, the focus is on the characteristic peak at mid-frequency region and the values are 194.8, 229.5, 218.1, and 236.4 Hz for *O. dillenii*, *T. indica*, mixture dye, and layer by layer co-sensitization solar cells, respectively. From this *O. dillenii* extract, DSSC has higher electron lifetime than all other devices which is consistent with I - V and EIS studies. The electron lifetime for all the devices is listed in Table 2. The mixture dye has higher electron lifetime than *T. indica* extract and as expected the layer by layer co-sensitization effect suppresses the effective electron hole pair generation in DSSC and gives lower electron lifetime. The electron lifetime in device fabricated using N719 dye exhibits higher value than the natural dye-based DSSCs and increases by ten folds. This is the reason why it produces higher V_{oc} and I_{sc} value than natural-based devices and produces higher efficiency.

Table 2 Photo electrochemical impedance parameters of various DSSCs estimated from EIS studies

Extract sources	Sheet resistance- R_s (Ω)	R_{ct2} (Ω)	Peak frequency- ω_{max} (Hz)	Electron lifetime- τ (s)
<i>O. dillenii</i>	18.36	238.48	194.8	8.1×10^{-4}
<i>T. indica</i>	21.18	668.47	229.5	6.9×10^{-4}
Mixture dye	21.81	357.91	218.1	7.3×10^{-4}
Layer by layer co-sensitization	20.17	805.65	236.4	6.7×10^{-4}
N719	24.47	54.54	15.3	10.6×10^{-3}

3.3.3 Incident photon-to-current efficiency studies

For further evaluation of the effectiveness of natural dyes in DSSC performance, the incident photon-to-current-efficiency for the solar cells is plotted in Fig. 12. IPCE is defined as the number of generated electrons divided by the number of incident photons, and it is known that it is dependent on the light harvesting efficiency and electron transfer yield which consists of the quantum charge injection and electron collection efficiency in the external circuit [50, 51]. At the frequency region between 400 and 475 nm and from 475 to 575 nm region, the *O. dilleni* extract shows the higher IPCE value of 25 and 15 %, respectively. *T. indica* extract shows higher IPCE value of around 12.5 % between 475 and 575 nm regions. The interesting fact about mixture dye is the continuous conversion of around 15 % between 450 and 550 nm region, and the spectral response is the combination of betalain and anthocyanin dyes. This result is consistent with UV–visible, *I*–*V*, and EIS results which showed that mixture dye has higher conversion efficiency than *T. indica* extract. Even though the spectral response of co-sensitization is the same as that of mixture dye, the IPCE value falls below 5 % which indicates that the suppression of photon generated electrons from the excited state of dye to the conduction band of current collecting electrode which attributes to lower IPCE value than all other natural dye-based DSSCs. For comparison, the DSSC was fabricated using N719 dye and the inset of Fig. 12. shows the IPCE spectrum which possesses around 80 % conversion efficiency between 475 and 575 nm regions. Therefore, the commercial dye-based DSSCs have been given higher

conversion efficiency than the natural dye-sensitized solar cells.

4 Conclusion

Successful conversion of solar radiation into electrical energy is achieved by betalain and anthocyanin dyes as a sensitizer in dye-sensitized solar cells. *O. dilleni* extract shows the maximum light conversion efficiency of 0.47 % than *T. indica* extract ($\eta = 0.14$ %) due to its better charge transfer between betalain dye molecule and TiO₂ surface. The sensitization of the mixture shows a moderate efficiency of 0.20 % which is 0.06 % higher than the anthocyanin dye-sensitized solar cell. Layer by layer co-sensitization results in lower efficiency compared to all other devices. Optimization of sensitizing time for individual dye is required to improve an overall conversion efficiency. Obviously, natural dyes exhibit lower photo-electrochemical activity than synthetic commercial dye. Nevertheless, natural dyes can be a green alternative, an eco-friendly, and a renewable energy source for the fabrication of dye-sensitized solar cells.

References

- Nazeeruddin MK, Baranoff E, Grätzel M (2011) Dye-sensitized solar cells: a brief overview. *Sol Energy* 85:1172–1178. doi:10.1016/j.solener.2011.01.018
- O'Regan B, Grätzel M (1991) A low-cost, high-efficiency solar cell based on dye-sensitized colloidal TiO₂ films. *Nature* 353:737–740. doi:10.1038/353737a0
- Lee J-K, Yang M (2011) Progress in light harvesting and charge injection of dye-sensitized solar cells. *Mater Sci Eng B* 176:1142–1160. doi:10.1016/j.mseb.2011.06.018
- Hagfeldt A, Boschloo G, Sun L et al (2010) Dye-sensitized solar cells. *Chem Rev* 110:6595–6663. doi:10.1002/chem.201101923
- Narayan MR (2012) Review: dye sensitized solar cells based on natural photosensitizers. *Renew Sustain Energy Rev* 16:208–215. doi:10.1016/j.rser.2011.07.148
- Zhou H, Wu L, Gao Y, Ma T (2011) Dye-sensitized solar cells using 20 natural dyes as sensitizers. *J Photochem Photobiol A Chem* 219:188–194. doi:10.1016/j.jphotochem.2011.02.008
- Liu B, Zhao X, Luo W (2008) The synergistic effect of two photosynthetic pigments in dye-sensitized mesoporous TiO₂ solar cells. *Dye Pigment* 76:327–331. doi:10.1016/j.dyepig.2006.09.004
- Park KH, Kim TY, Park JY et al (2013) Photochemical properties of dye-sensitized solar cell using mixed natural dyes extracted from *Gardenia Jasminoide* Ellis. *J Electroanal Chem* 689:21–25. doi:10.1016/j.jelechem.2012.11.026
- Patrocínio AOT, Mizoguchi SK, Paterno LG et al (2009) Efficient and low cost devices for solar energy conversion: efficiency and stability of some natural-dye-sensitized solar cells. *Synth Met* 159:2342–2344. doi:10.1016/j.synthmet.2009.08.027
- Calogero G, Di Marco G, Cazzanti S et al (2010) Efficient dye-sensitized solar cells using red turnip and purple wild Sicilian

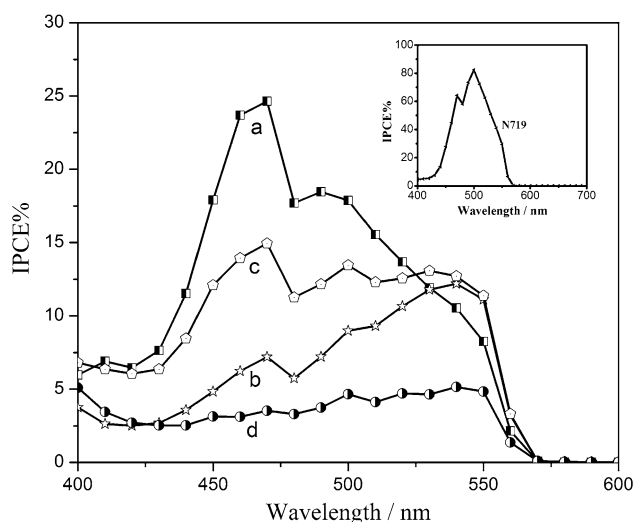


Fig. 12 Comparison of IPCE spectra of DSSCs fabricated using *a* *O. dilleni*, *b* *T. indica*, *c* the mixture, and *d* co-sensitization process. Inset shows the IPCE spectrum of DSSC constructed using N719 dye

- prickly pear fruits. *Int J Mol Sci* 11:254–267. doi:10.3390/ijms11010254
11. Strack D, Vogt T, Schliemann W (2003) Recent advances in betalain research. *Phytochemistry* 62:247–269. doi:10.1016/S0031-9422(02)00564-2
 12. Castellar MR, Obón JM, Alacid M, Fernández-López JA (2008) Fermentation of *Opuntia stricta* (Haw.) fruits for betalains concentration. *J Agric Food Chem* 56:4253–4257. doi:10.1021/jf703699c
 13. Chang SF, Hsieh CL, Yen GC (2008) The protective effect of *Opuntia dillenii* Haw fruit against low-density lipoprotein peroxidation and its active compounds. *Food Chem* 106:569–575. doi:10.1016/j.foodchem.2007.06.017
 14. Davies K (2009) Annual plant reviews, plant pigments and their manipulation. Wiley, Hoboken
 15. Singh AMBG, Durai A, Murugesan S (2012) Evaluation of colour and stability of anthocyanin in red tamarind (*Tamarindus indica* L). *Int J Adv Life Sci (IJALS)* 5:137–144
 16. Ludin NA, Al-Alwani Mahmoud AM, Bakar Mohamad A et al (2014) Review on the development of natural dye photosensitizer for dye-sensitized solar cells. *Renew Sustain Energy Rev* 31:386–396. doi:10.1016/j.rser.2013.12.001
 17. Gokilamani N, Muthukumarasamy N, Thambidurai M et al (2014) Basella alba rubra spinach pigment-sensitized TiO₂ thin film-based solar cells. *Appl Nanosci*. doi:10.1007/s13204-014-0317-2
 18. Hemmatzadeh R, Mohammadi A (2013) Improving optical absorptivity of natural dyes for fabrication of efficient dye-sensitized solar cells. *J Theor Appl Phys* 57:1–7. doi:10.1186/2251-7235-7-57
 19. Isah KU, Ahmadu U, Idris A et al (2015) Betalain pigments as natural photosensitizers for dye-sensitized solar cells: the effect of dye pH on the photoelectric parameters. *Mater Renew Sustain Energy* 4:39. doi:10.1007/s40243-014-0039-0
 20. Sengupta D, Mondal B, Mukherjee K (2015) Visible light absorption and photo-sensitizing properties of spinach leaves and beetroot extracted natural dyes. *Spectrochim Acta Part A Mol Biomol Spectrosc* 148:85–92. doi:10.1016/j.saa.2015.03.120
 21. Thankappan A, Divya S, Augustine AK et al (2015) Highly efficient betanin dye based ZnO and ZnO/Au Schottky barrier solar cell. *Thin Solid Films* 583:102–107. doi:10.1016/j.tsf.2015.03.052
 22. Zolkepli Z, Lim A, Ekanayake P, Tennakoon K (2015) Efficiency enhancement of cocktail dye of *Ixora coccinea* and *Tradescantia spathacea* in DSSC. *J Biophys* 2015:1–8. doi:10.1155/2015/582091
 23. Adel R, Abdallah T, Moustafa YM et al (2015) Effect of polymer electrolyte on the performance of natural dye sensitized solar cells. *Superlattices Microstruct* 86:62–67. doi:10.1016/j.spmi.2015.07.024
 24. Chien CY, Hsu BD (2013) Optimization of the dye-sensitized solar cell with anthocyanin as photosensitizer. *Sol Energy* 98:203–211. doi:10.1016/j.solener.2013.09.035
 25. Lim A, Pg Damit DNFB, Ekanayake P (2015) Tailoring of extraction solvent of *Ixora coccinea* flower to enhance charge transport properties in dye-sensitized solar cells. *Ionics (Kiel)* 21:2897–2904. doi:10.1007/s11581-015-1489-9
 26. Munawaroh H, Adillah GF, Saputri LNMZ et al (2016) The copigmentation of anthocyanin isolated from mangosteen pericarp (*Garcinia Mangostana* L.) as natural dye for dye-sensitized solar cells (DSSC). *IOP Conf Ser Mater Sci Eng* 107:012061. doi:10.1088/1757-899X/107/1/012061
 27. Prima EC, Al Qibtiya M, Yuliarto B et al (2016) Influence of anthocyanin co-pigment on electron transport and performance in black rice dye-sensitized solar cell. *Ionics (Kiel)*. doi:10.1007/s11581-016-1673-6
 28. Reda A, Tadesse S, Yohannes T (2014) Dye-sensitized solar cell using natural dyes extracted from *Morus atba* Lam fruit and *Striga hermonthica* flower. *J Photonics Energy* 4:043091. doi:10.1117/1.JPE.4.043091
 29. Isah Kimpa M (2012) Photoelectric characterization of dye sensitized solar cells using natural dye from pawpaw leaf and flame tree flower as sensitizers. *Mater Sci Appl* 03:281–286. doi:10.4236/msa.2012.35041
 30. Zhang D, Lanier SM, Downing JA et al (2008) Betalain pigments for dye-sensitized solar cells. *J Photochem Photobiol A Chem* 195:72–80. doi:10.1016/j.jphotochem.2007.07.038
 31. Kumara NTRN, Ekanayake P, Lim A et al (2013) Layered co-sensitization for enhancement of conversion efficiency of natural dye sensitized solar cells. *J Alloys Compd* 581:186–191. doi:10.1016/j.jallcom.2013.07.039
 32. Hao S, Wu J, Huang Y, Lin J (2006) Natural dyes as photosensitizers for dye-sensitized solar cell. *Sol Energy* 80:209–216. doi:10.1016/j.solener.2005.05.009
 33. Wongcharee K, Meeyoo V, Chavadej S (2007) Dye-sensitized solar cell using natural dyes extracted from rosella and blue pea flowers. *Sol Energy Mater Sol Cells* 91:566–571. doi:10.1016/j.solmat.2006.11.005
 34. Polo A, Murakamiha N (2006) Blue sensitizers for solar cells: natural dyes from Calafate and Jaboticaba. *Sol Energy Mater Sol Cells* 90:1936–1944. doi:10.1016/j.solmat.2006.02.006
 35. Hernandez-Martinez AR, Estevez M, Vargas S et al (2011) New dye-sensitized solar cells obtained from extracted bracts of *Bougainvillea glabra* and *spectabilis* betalain pigments by different purification processes. *Int J Mol Sci* 12:5565–5576. doi:10.3390/ijms12095565
 36. Calogero G, Di Marco G (2008) Red Sicilian orange and purple eggplant fruits as natural sensitizers for dye-sensitized solar cells. *Sol Energy Mater Sol Cells* 92:1341–1346. doi:10.1016/j.solmat.2008.05.007
 37. Oprea CI, Dumbravă A, Enache I et al (2012) A combined experimental and theoretical study of natural betalain pigments used in dye-sensitized solar cells. *J Photochem Photobiol A Chem* 240:5–13. doi:10.1016/j.jphotochem.2012.05.003
 38. Narayan M, Raturi A (2011) Investigation of some common Fijian flower dyes as photosensitizers for dye sensitized solar cells abstract. *Appl Sol Energy* 47:112–117. doi:10.3103/S0003701X11020149
 39. Sandquist C, McHale JL (2011) Improved efficiency of betanin-based dye-sensitized solar cells. *J Photochem Photobiol A Chem* 221:90–97. doi:10.1016/j.jphotochem.2011.04.030
 40. Cherepy NJ, Smestad GP, Grätzel M, Zhang JZ (1997) Ultrafast electron injection: implications for a photoelectrochemical cell utilizing an anthocyanin dye-sensitized TiO₂ nanocrystalline electrode. *J Phys Chem B* 101:9342–9351. doi:10.1021/jp972197w
 41. Hemalatha KV, Karthick SN, Justin Raj C et al (2012) Performance of *Kerria japonica* and *Rosa chinensis* flower dyes as sensitizers for dye-sensitized solar cells. *Spectrochim Acta Part A Mol Biomol Spectrosc* 96:305–309. doi:10.1016/j.saa.2012.05.027
 42. Calogero G, Yum J-H, Sinopoli A et al (2012) Anthocyanins and betalains as light-harvesting pigments for dye-sensitized solar cells. *Sol Energy* 86:1563–1575. doi:10.1016/j.solener.2012.02.018
 43. Chang H, Lo Y-J (2010) Pomegranate leaves and mulberry fruit as natural sensitizers for dye-sensitized solar cells. *Sol Energy* 84:1833–1837. doi:10.1016/j.solener.2010.07.009
 44. Chang H, Wu HM, Chen TL et al (2010) Dye-sensitized solar cell using natural dyes extracted from spinach and ipomoea. *J Alloys Compd* 495:606–610. doi:10.1016/j.jallcom.2009.10.057

45. Furukawa S, Iino H, Iwamoto T et al (2009) Characteristics of dye-sensitized solar cells using natural dye. *Thin Solid Films* 518:526–529. doi:[10.1016/j.tsf.2009.07.045](https://doi.org/10.1016/j.tsf.2009.07.045)
46. Hug H, Bader M, Mair P, Glatzel T (2014) Biophotovoltaics: natural pigments in dye-sensitized solar cells. *Appl Energy* 115:216–225. doi:[10.1016/j.apenergy.2013.10.055](https://doi.org/10.1016/j.apenergy.2013.10.055)
47. Lai WH, Su YH, Teoh LG, Hon MH (2008) Commercial and natural dyes as photosensitizers for a water-based dye-sensitized solar cell loaded with gold nanoparticles. *J Photochem Photobiol A Chem* 195:307–313. doi:[10.1016/j.jphotochem.2007.10.018](https://doi.org/10.1016/j.jphotochem.2007.10.018)
48. Lim A, Kumara NTRN, Tan AL et al (2015) Potential natural sensitizers extracted from the skin of *Canarium odontophyllum* fruits for dye-sensitized solar cells. *Spectrochim Acta Part A Mol Biomol Spectrosc* 138:596–602. doi:[10.1016/j.saa.2014.11.102](https://doi.org/10.1016/j.saa.2014.11.102)
49. Luo P, Niu H, Zheng G et al (2009) From salmon pink to blue natural sensitizers for solar cells: *Canna indica* L., *Salvia splendens*, cowberry and *Solanum nigrum* L. *Spectrochim Acta Part A Mol Biomol Spectrosc* 74:936–942. doi:[10.1016/j.saa.2009.08.039](https://doi.org/10.1016/j.saa.2009.08.039)
50. Li W, Jin G, Hu H et al (2015) Phosphotungstic acid and WO₃ incorporated TiO₂ thin films as novel photoanodes in dye-sensitized solar cells. *Electrochim Acta* 153:499–507. doi:[10.1016/j.electacta.2014.12.030](https://doi.org/10.1016/j.electacta.2014.12.030)
51. Motlak M, Barakat NAM, Akhtar MS et al (2015) High-efficiency dye-sensitized solar cells based on nitrogen and graphene oxide co-incorporated TiO₂ nanofibers photoelectrode. *Chem Eng J* 268:153–161. doi:[10.1016/j.cej.2015.01.065](https://doi.org/10.1016/j.cej.2015.01.065)